Pharmaceutical Research, Vol. 24, No. 3, March 2007 (© 2007)
DOI: 10.1007/s11095-006-9178-z

Research Paper

Glycine Crystallization in Frozen and Freeze-dried Systems: Effect of pH and Buffer Concentration

Dushyant B. Varshney,[1,2,6] Satyendra Kumar,[3] Evgenyi Y. Shalaev,[4] Prakash Sundaramurthi,[1] Shin-Woong Kang,[5] Larry A. Gatlin,[4] and Raj Suryanarayanan[1,6]

Received August 3, 2006; accepted October 11, 2006; published online January 24, 2007

Purpose. (1) To determine the effect of solution pH before lyophilization, over the range of 1.5 to 10, on the salt and polymorphic forms of glycine crystallizing in frozen solutions and in lyophiles. (2) To quantify glycine crystallization during freezing and annealing as a function of solution pH before lyophilization. (3) To study the effect of phosphate buffer concentration on the extent of glycine crystallization before and after annealing.
Materials and Methods. Glycine solutions (10% w/v), with initial pH ranging from 1.5 to 10, were cooled to −50°C, and the crystallized glycine phases were identified using a laboratory X-ray source. Over the same pH range, glycine phases in lyophiles obtained from annealed solutions (0.25, 2 and 10% w/v glycine), were characterized by synchrotron X-ray diffractometry (SXRD). In the pH range of 3.0 to 5.9, the extent of glycine crystallization during annealing was monitored by SXRD. Additionally, the effect of phosphate buffer concentration (50 to 200 mM) on the extent of glycine crystallization during freezing, followed by annealing, was determined.
Results. In frozen solutions, β-glycine was detected when the initial solution pH was ≥4. In the lyophiles, in addition to β- and γ-glycine, glycine HCl, diglycine HCl, and sodium glycinate were also identified. In the pH range of 3.0 to 5.9, decreasing the pH reduced the extent of glycine crystallization in the frozen solution. When the initial pH was fixed at 7.4, and the buffer concentration was increased from 50 to 200 mM, the extent of glycine crystallization in frozen solutions decreased with an increase in buffer concentration.
Conclusion. Both solution pH and solute concentration before lyophilization influenced the salt and polymorphic forms of glycine crystallizing in frozen solutions and in lyophiles. The extent of glycine crystallization in frozen solutions was affected by the initial pH and buffer concentration of solutions. The high sensitivity of SXRD allowed simultaneous detection and quantification of multiple crystalline phases.

KEY WORDS: freeze-drying; glycine; lyophiles; phosphate buffer; polymorphs and salts; synchrotron XRD.

INTRODUCTION

Lyophilization (freeze-drying) is widely utilized for manufacturing pharmaceutical proteins, diagnostic agents and other thermolabile therapeutic agents. Lyophilized formulations are multi-component systems containing the active pharmaceutical ingredient (API) and excipients such as bulking agents, lyoprotectants and buffers. The physical form of the API and the excipients in the final lyophile will influence the product stability (chemical as well as physical) and performance (e.g., reconstitution time) (1–4). In protein formulations, a major challenge is to minimize the damage to protein from the stresses (e.g., pH changes, increase solute concentration, dehydration) experienced during the freeze-drying cycle. Amorphous sugars (e.g., sucrose, trehalose) provide lyoprotection during freeze drying and subsequent storage. Crystalline bulking agents (e.g., glycine) enable primary drying at elevated temperatures and therefore decreasing the cycle time and also result in elegant lyophiles (1–9).

The physical state of the formulation components in the final lyophiles will be determined by the composition of the dosage form, as well as the processing conditions. Solute as well as ice crystallization can often be induced by annealing frozen solutions (6–13). Pikal-Cleland *et al.* demonstrated a decrease in crystallization of disodium hydrogen phosphate buffer (initial concentration 10 mM) in the presence of amorphous glycine (initial concentration 50 mM). Interest-

[1] Department of Pharmaceutics, College of Pharmacy, University of Minnesota, Minneapolis, Minnesota 55455, USA.
[2] Present address: Eli Lilly and Company, Lilly Corporate Center, Indianapolis, Indiana 46285, USA.
[3] Division for Materials Research, National Science Foundation, 4201 Wilson Blvd, Arlington, Virginia 22230, USA.
[4] Pfizer Groton Laboratories, Groton, Connecticut 06340, USA.
[5] Department of Physics, Kent State University, Kent, Ohio 44242, USA.
[6] To whom correspondence should be addressed. (e-mail: varshneydu@lilly.com and surya001@umn.edu)

ingly, when the initial glycine concentration was >100 mM, the crystallization of buffer salt was facilitated (14). Pyne *et al.* demonstrated a complex interplay between the amorphous and crystalline phases in the ternary system composed of mannitol, glycine and sodium phosphate (12). The crystallization of buffer salts (e.g., in the case of sodium phosphate buffer) in frozen systems is not desired due to the potential for significant pH-shifts that can affect the protein stability (7,14–16). In this context, to develop a robust process, it is important to: (a) identify the phase transitions of formulations components, and (b) investigate the extent of crystallization, at different stages of freeze-drying cycle.

In the case of glycine, the formulation components including the API can inhibit or enhance the crystallization of glycine during freezing (9–12,14). Moreover, the solution pH before lyophilization, can influence the extent of glycine crystallization and also the salt and polymorphic forms of glycine. The isoelectric pH of glycine ($^{+}H_3NCH_2COO^{-}$) is 5.97. The pKa values of 2.35 (carboxylic acid) and 9.78 (amine), dictate the speciation and solubility of glycine forms as a function of pH (17–21).

The crystallization behavior of glycine from aqueous solutions has been widely studied (21–25). At ambient conditions, neutral glycine exists in three polymorphic forms, with the order of their thermodynamic stability being $\gamma > \alpha > \beta$. While α- and γ-glycine are enantiotropically related, β-glycine is monotropically related to α- and γ-glycine. Although γ-glycine is the stable form at room temperature, α-glycine readily crystallizes from solutions. While γ-glycine can be crystallized from acidic or basic solutions, the metastable β-glycine is known to crystallize from water–alcohol mixtures, or from highly supersaturated solutions. Controlled cooling of neutral glycine solutions yielded β-glycine as a eutectic mixture with ice characterized by the melting temperature of ~ −4°C. Upon exposure to moisture at ambient temperature, β-glycine readily converted to a mixture of α- and γ-glycine.

In addition to the widespread interest in the crystallization of glycine from solutions, in recent years, considerable attention has been paid to the *process-induced phase transitions* of glycine polymorphs (17,22–30). Towler *et al.* elegantly demonstrated the impact of pH-dependent molecular speciation and the role of counterions upon $\alpha \rightarrow \gamma$ polymorphic transition (17). Yu and Ng determined the effect of initial pH (range 1.7 to 10) on the crystallization of glycine polymorphs and salts upon spray-drying (27). While neutral glycine solutions produced α-glycine, γ-glycine was obtained by adjusting the pH to 3, 4, 8 or 9. Pioneering studies by Akers *et al.* demonstrated the effect of glycine salts, initial solution pH, and ionic strength on the glycine crystallization in frozen solutions and lyophiles (28). Although crystallization of γ-glycine was evident at pH 3, a mixture of β-glycine and sodium glycinate was observed at pH 10. The effect of processing conditions (e.g., cooling rate, annealing) have been studied mostly in *neutral* glycine solutions. Chongprasert *et al.* utilized low-temperature differential scanning calorimetry (DSC) and freeze-drying microscopy to investigate the thermal behavior of glycine (29), while Pyne and Suryanarayanan used low-temperature X-ray diffractometry (XRD) to study the phase transitions of glycine in frozen aqueous solutions and during freeze-drying (30).

Although Akers *et al.* studied the crystallization of glycine when solutions of selected pH values were cooled, there is no report on the crystallization behavior of glycine in frozen solutions and lyophiles obtained from solutions over the entire pH range of 1 to 10. Moreover, no attempts have been made to quantify the crystalline glycine content, during different stages of the freeze-drying cycle, both in the presence and absence of buffer.

It is known that the crystallization of the base component of phosphate buffer as disodium hydrogen phosphate dodecahydrate (DHPD) causes pH shifts in frozen solutions (31,32). Pronounced pH shifts of up to three units were observed when the initial buffer concentrations were ≥50 mM (31–33). In our previous report, using synchrotron X-ray diffractometry (SXRD), we have demonstrated the effect of initial solute concentration (ranging from 1 to 100 mM) on the selective crystallization of DHPD (33). Gomez *et al.* developed an elegant method to monitor pH changes at temperatures ≥ −17°C by using a low temperature electrode (31,32). Unfortunately, this approach will not be suitable to monitor the pH at the temperature of our interest (~ −50°C), and also during drying. To this end, SXRD can be utilized for quantification of crystalline phases that are responsible for causing such pH-shifts (33). Alternative methods are being developed to monitor shift in acidity induced by freeze-drying. Govindarajan *et al.* utilized sulfonephthalein dyes and diffuse reflectance visible spectroscopy to evaluate the acidity of trehalose–citrate lyophiles (34).

We have demonstrated the utility and power of SXRD to detect solute crystallization from dilute solutions (33). Synchrotron radiation has already shown promise for *in situ* monitoring of crystallization, investigating solution mediated polymorphic transformations, and for quantifying the crystallinity in a substantially amorphous matrix (35–37). In addition to high sensitivity, very rapid data collection is possible (<1 s) enabling time-resolved studies (33,35–37). An approach based on SXRD could offer numerous advantages. (1) Reliable, unambiguous and simultaneous detection of multiple solid phases crystallizing from solution. The high sensitivity enables detection of even minor formulation components such as buffer salts. (2) Quantification of analyte crystallinity in complex, multi-component systems. (3) Capability to monitor phase transitions *during* the entire freeze-drying cycle.

In this investigation we had three objectives. (1) To determine the effect of initial solution pH, over the range of 1.5 to 10, on the salt and polymorphic forms of glycine crystallizing in frozen solutions and upon subsequent lyophilization. In the same pH range, the effect of solute concentration, ranging from 0.25 to 10% w/v (33 to 1332 mM), was also determined. (2) To determine the effect of annealing on the extent of glycine crystallization in frozen solutions. The initial solution pH ranged from 3.0 to 5.9. (3) Finally to investigate the effect of phosphate buffer concentration, over the range of 50 to 200 mM, on the extent of glycine crystallization before and after annealing. While the studies were initiated with a laboratory-based X-ray diffractometer, the complexity of the system, the presence of multiple crystalline phases and low analyte concentrations necessitated the use of synchrotron radiation for most of the studies.

MATERIALS AND METHODS

Materials

Glycine, sodium glycinate, disodium hydrogen phosphate (Na_2HPO_4) and monosodium dihydrogen phosphate (NaH_2PO_4) were obtained from Sigma, and used without further purification. In all experiments deionized water was used to prepare solutions. A pH meter (Oakton), calibrated with standard buffer solutions (Oakton standard buffers; pH 1.68, 4.01, 7.00 and 10.00; certified by NIST) was used.

Preparation of Glycine and Buffer Solutions

Aqueous glycine solutions (0.25, 2 and 10% w/v), ranging in pH from 1.5 to 5 and 7 to 10, were prepared (Table I). The pH was adjusted by adding 1, 2 or 5 M HCl/NaOH solutions. There was no significant change in the concentration as very small volumes of acid/base were required to attain the desired pH values. Phosphate-buffered (200/100/50 mM) glycine (2% w/v) solutions were prepared by dissolving appropriate amounts of glycine and sodium phosphate buffer (Na_2HPO_4:NaH_2PO_4; 9:1 w/w ratio) in 50 ml deionized water. The final pH of 7.4 (±0.01) of all the solutions was confirmed experimentally. The solutions were filtered (45 μm nylon filter) and stored in tightly closed scintillation vials in dark, at room temperature (RT).

Preparation of Lyophiles

Lyophilization was carried out in a bench-top (VirTis® AdVantage™, Gardiner, NY) freeze dryer. Glass vials (USP Type I borosilicate, VWR®) with 20 mm neck size and 10 ml fill volume were used. The vials were filled with glycine solutions (5 ml) of various concentrations and pH values, and then loaded into the freeze dryer (Table I). The solutions were cooled to a shelf temperature of −50°C at 1°C/min, held for 1.5 h, heated to −20°C and annealed for 4 h. Primary drying (at 60 mTorr) was carried out at a shelf temperature of −30°C for 30 h. Secondary drying was first conducted at −10°C for 3 h and then at 10°C for 5 h. At the end of lyophilization cycle, the vials were capped using rubber stoppers (two-leg gray butyl, Fisher Scientific) under vacuum (at 60 mTorr) and then stored in the dark, at RT.

The cooling rate of 1°C/min and other process variables during freeze-drying were selected based on: (1) the number of vials (30 in each batch) and the sample volume (5 ml in each vial), (2) results of preliminary *in situ* laboratory XRD experiments (not discussed in the paper) wherein the entire freeze-drying cycle was simulated and (3) the thermal transitions in frozen glycine solutions (28–30). The eutectic melt in frozen aqueous glycine solutions was observed at ~−4°C. At annealing temperatures ≥−10°C, polymorphic transition was observed in the crystalline glycine. The conclusions were based on both DSC and low-temperature XRD (28–30). Therefore, we selected the annealing (−20°C) and primary drying temperatures (−30°C) to be substantially below these transition temperatures.

Table I describes the compositions of the sample solutions, the processing conditions and the XRD method used for analysis.

Methods

Laboratory X-ray Diffractometry

A powder X-ray diffractometer (Model XDS 2000, Scintag; Bragg-Brentano focusing geometry) with a variable temperature stage (High-Tran Cooling System, Micristar, Model 828D, R.G. Hansen & Associates; working temperature range: −190 to 300°C) and a solid-state detector was utilized for low-temperature studies. The glycine solution (200 μL) was pipetted into a copper sample holder, covered with a stainless steel dome with a beryllium window, and cooled at

Table I. Composition of Sample Solutions, Processing Conditions and Method of Analysis

Solute(s)	Initial pH	Initial Concentration	Total Number of Samples	Processing Condition	XRD Conducted on[a]	Radiation
Glycine	1.5, 2.0, 3.0, 4.0, 5.0, 5.9, 7.0, 8.0, 9.0, 10.0	10% w/v (1332 mM)	10	Freezing (2°C/min)	Frozen solutions	Laboratory source
		10% w/v (1332 mM)	10	Freezing (1-C/min), annealing and drying	Final lyophiles	Synchrotron source
		2% w/v (266 mM)	10			
		0.25% w/v (33 mM)	10			
Glycine	3.0, 4.0, 5.0, 5.9	2% w/v (266 mM)	4	Freezing (10°C/min) and annealing	Frozen and annealed solutions	Synchrotron source
Glycine + Sodium phosphate buffer	7.4	A) 266 mM + 200 mM	3			
		B) 266 mM + 100 mM				
		C) 266 mM + 50 mM				

[a] The stage of the freeze-drying cycle at which the characterization studies were performed.

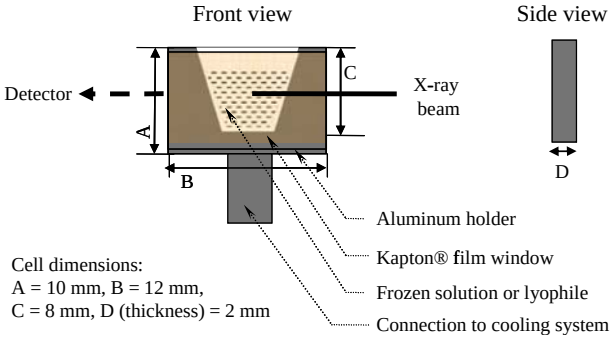

Fig. 1. Schematic diagram of the sample cell used for SXRD experiments.

2°C/min, from RT to −50°C and held for 15 min. It was then exposed to CuKα radiation (45 kV × 40 mA) and the XRD patterns were obtained by scanning over a 2θ angular range of 2 to 45° with a step size of 0.05° and a dwell time of 1 s.

Synchrotron XRD (Transmission Mode)

The experiments were performed at the synchrotron beam line 6-ID-B of the Midwest Universities Collaborative Team's Sector 6, at the Advanced Photon Source, Argonne National Laboratory (Argonne, IL, USA). The variable temperature stage (High-Tran Cooling System,) was attached to the Eulerian cradle (Huber 512) using an aluminum (Al) plate. A monochromatic X-ray beam (0.76534 Å; beam size 100 (vertical) × 200 (horizontal) μm) was used. A triple-bounce channel-cut Si single crystal monochromator with [111] faces polished was used as the monochromator which limited the line broadening to its theoretical low limit, i.e., the Darwin width.

The flux of the incident X-rays (intensity: 10^{13} photons/sec/mrad^2/mm^2) was attenuated to prevent detector saturation. An image plate detector (MAR3450) with 3450 × 3,450 pixel resolution in 34.5 mm diameter area with a readout time of 108 s (best resolution mode) was used. The sample-to-detector distance was set to 500.1 mm. The calibration was performed using a silicon standard (SRM 640b, NIST). Time-resolved two-dimensional (2D) data were integrated to yield one-dimensional (1D) d-spacing (Å) or 2θ (°) scans using the FIT2D software developed by A. P. Hammersley of the European Synchrotron Radiation Facility (38,39). A commercial software (JADE, version 7.1, Materials Data, Inc.) package was used for determining the integrated peak intensities.

Glycine or buffered glycine solution (200 μL) was placed in a specially designed Al sample cell with a Kapton® window (Fig. 1). The entire setup was covered with a stainless steel dome with a beryllium window. The solutions were cooled at 2

Table II. Distribution of Glycine Polymorphs and Salts in Frozen Solutions and in the Final Lyophiles as a Function of Initial pH and Concentration

Initial Glycine Concentration (% w/v) ↓	Initial pH of Solution →									
	1.5	2	3	4	5	5.9[a]	7	8	9	10
10[b]	G.HCl	DiG.HCl + G.HCl	DiG.HCl	β + DiG.HCl	β + DiG.HCl	β	β	β	β	–
10[c]	G.HCl	DiG.HCl + G.HCl	γ + DiG.HCl	β+ DiG.HCl (trace)	β+ DiG.HCl (trace)	β	β	γ	γ + G.Na	γ + G.Na
2[c]	G.HCl+ DiG.HCl (trace)	DiG.HCl + G.HCl	γ+ β+ DiG.HCl (trace)	β+ DiG.HCl (trace) + γ (trace)	β+ DiG.HCl (trace) + γ (trace)	β	β+ γ (trace)	γ+ G.Na (trace)	γ+ G.Na (trace)	γ + G.Na
0.25[c]	G.HCl+ DiG.HCl (trace)	G.HCl+ DiG.HCl (minor)	γ + β + DiG.HCl	β+ DiG.HCl (minor)	β+ DiG.HCl (minor)	β	β	β	γ+ G.Na (minor)	γ+ G.Na (minor)

[a] pH of neutral glycine solution
[b] frozen solutions studied using laboratory XRD (major phase in all case = hexagonal ice)
[c] final lyophiles studied using synchrotron XRD
G.HCl = glycine hydrochloride
DiG.HCl = diglycine hydrochloride
G.Na = sodium glycinate
β = beta glycine
γ = gamma glycine
minor = percent intensity of the characteristic peaks with respect to the most intense peak was between 0.2–0.5%
trace = percent intensity of the characteristic peaks with respect to the most intense peak <0.2%

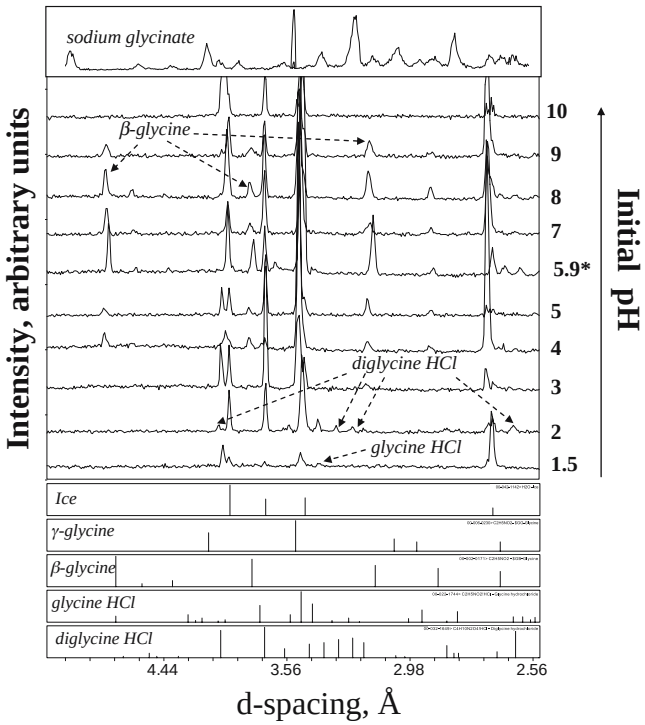

Fig. 2. Laboratory XRD patterns of *frozen solutions* of glycine with initial pH in the range of 1.5 to 10. In each case, 10% (w/v) glycine solution was cooled at 2°C/min from RT to −50°C and held for 15 min. Initial pH = measured pH of the solutions before lyophilization. *Asterisk*: pH of neutral glycine solution. For comparison purposes, the stick patterns of ice, β-glycine, γ-glycine, glycine HCl , diglycine HCl obtained from the Powder Diffraction Files of the International Centre for Diffraction Data (40,42), and laboratory XRD pattern of sodium glycinate (*Sigma*) are provided. The results are summarized in Table II.

or 10°C/min from RT to −50°C, held for 15 min and annealed at −20°C for 20 mins. The frozen solutions were exposed to high-intensity X-ray beam (total transmission: 3.44×10^{-2} KeV, exposure time: 5/10 s) at different stages of freezing and annealing. Additionally, a blank/background reading was obtained by exposing an empty sample cell to X-ray beam. The lowest controlled cooling rate in the variable temperature stage was 2°C/min. A higher cooling rate of 10°C/min was used for solutions that were subsequently annealed. The final lyophiles of glycine were placed in the sample cell (Fig. 1) and exposed to synchrotron radiation (with total transmission: 5.71×10^{-4} KeV, exposure times of 1–10 s).

XRD Data Analysis

The data, obtained either from the laboratory or the synchrotron source, was analyzed using a commercial software package (JADE, version 7.1, Materials Data, Inc.). The peaks in the 1D-XRD patterns were integrated and a plot of the integrated intensity (counts) as a function of d-spacing (Å) was obtained in each case. The results were compared with the published data in the Powder Diffraction Files (PDF) of the International Centre for Diffraction Data (ICDD) card patterns. This formed the basis for the assignment of major and minor phases shown in Table II. To obtain Figs. 2 to 5, the relevant XRD patterns were overlaid and compared with the standard stick patterns of crystalline glycine phases and ice (40,42).

RESULTS AND DISCUSSION

The 'as is' glycine was identified as the α-polymorph, based on XRD, DSC and thermogravimetric analysis.

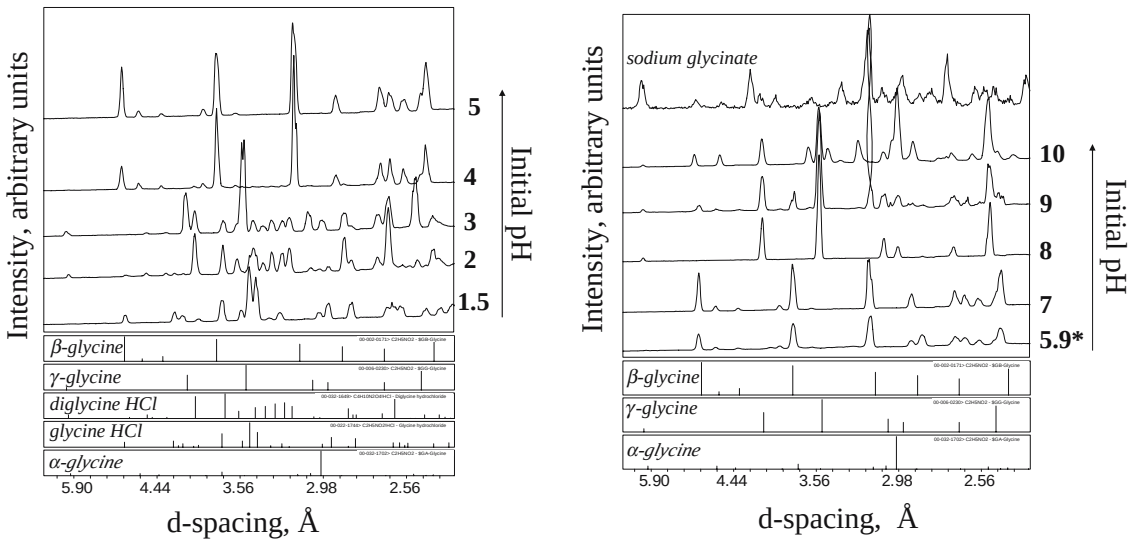

Fig. 3. 1D-SXRD patterns of *final lyophiles* of glycine with initial solution pH in the range of 1.5 to 10. In each case, 10% (w/v) glycine solution was cooled at 1°C/min from RT to −50°C and held for 15 min in the freezing stage. Initial pH = measured pH of the solutions before lyophilization. *Asterisk*: pH of neutral glycine solution. For comparison purposes, the stick patterns of: β-glycine, γ-glycine, α-glycine, glycine HCl and diglycine HCl (42); and laboratory XRD pattern of sodium glycinate (*Sigma*) are provided. The results are summarized in Table II.

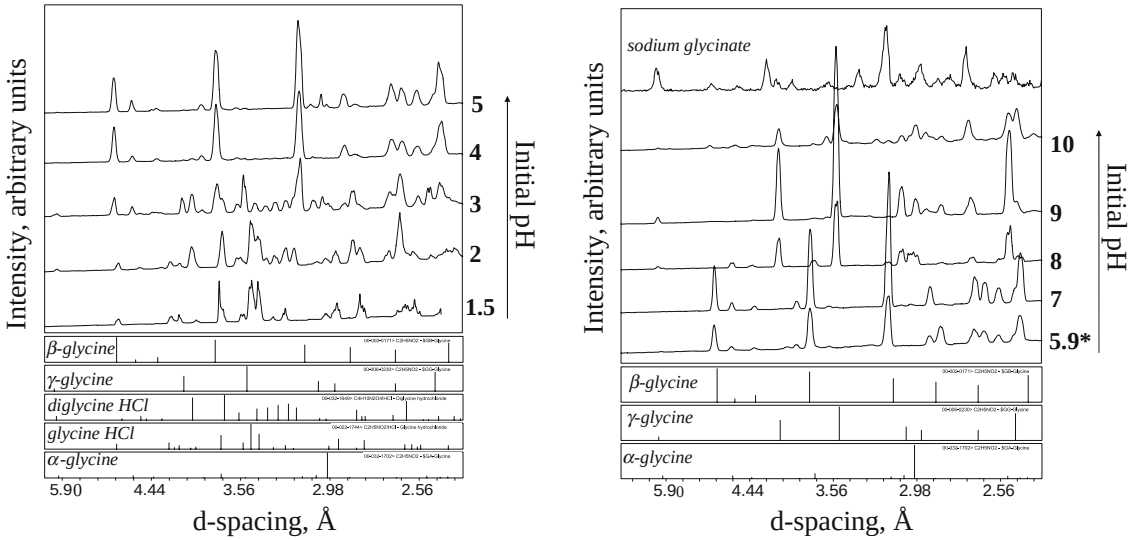

Fig. 4. 1D-SXRD patterns of *final lyophiles* of glycine with initial solution pH in the range of 1.5 to 10. In each case, 2% (w/v) glycine solution was cooled at 1°C/min from RT to −50°C and held for 15 min in the freezing stage. Initial pH = measured pH of the solutions before lyophilization. *Asterisk*: pH of neutral glycine solution. For comparison purposes, the stick patterns of: β-glycine, γ-glycine, α-glycine, glycine HCl and diglycine HCl (42); and laboratory XRD pattern of sodium glycinate are provided. The results are summarized in Table II.

Glycine Crystallization in Frozen Solutions and Lyophiles—Effects of Solution pH and Concentration

Table II lists the different polymorphs and salts of glycine identified in the frozen solutions and in the lyophiles. While the frozen solutions were characterized by laboratory XRD, the high sensitivity of SXRD was utilized to detect the crystalline phases in the lyophiles. The β- and γ-polymorphic forms of glycine ($^{+}H_3NCH_2CO_2^{-}$) were characterized by their unique lines with d-spacings of 4.92 and 4.07 Å, respectively. Glycine hydrochloride (G.HCl, $^{+}H_3NCH_2CO_2H{\cdot}Cl^{-}$) and diglycine hydrochloride (DiG.HCl, $^{+}H_3NCH_2CO_2^{-}{\cdot}^{+}H_3NCH_2CO_2H{\cdot}Cl^{-}$) were characterized by their unique lines with d-spacings of 3.48 and 3.98 Å, respectively. SXRD enabled the detection of 'minor' and 'trace' phases. For the purpose of this discussion, a phase is considered 'minor' and 'trace' when the percent intensity of the characteristic peak with respect to the most intense peak was between 0.2–0.5 and < 0.2%, respectively (Table II).

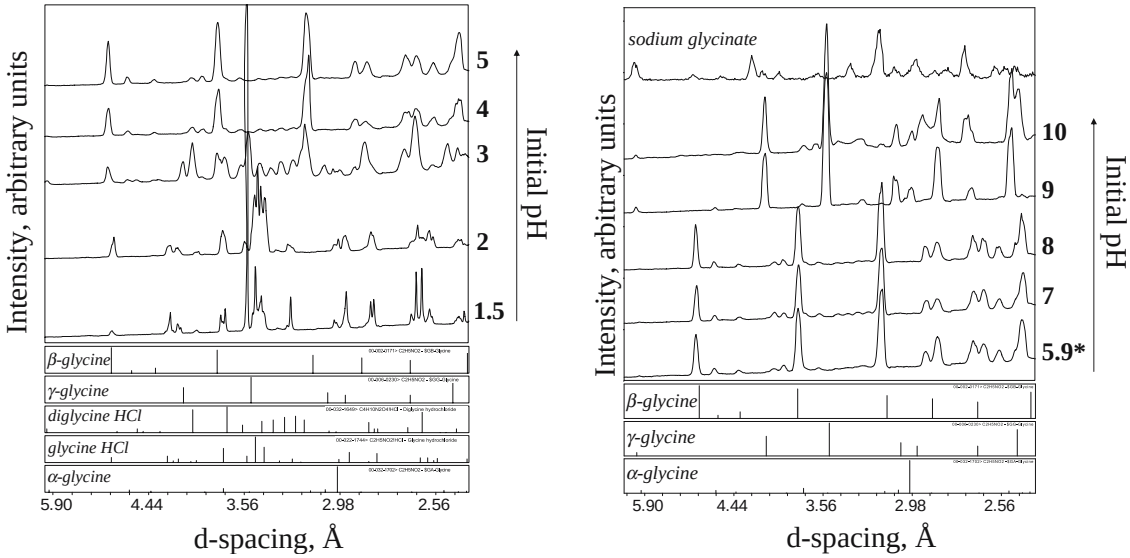

Fig. 5. 1D-SXRD patterns of *final lyophiles* of glycine with initial solution pH in the range of 1.5 to 10. In each case, 0.25% (w/v) glycine solution was cooled at 1°C/min from RT to −50°C and held for 15 min in the freezing stage. Initial pH = measured pH of the solutions before lyophilization. *Asterisk*: pH of neutral glycine solution. For comparison purposes, the stick patterns of: β-glycine, γ-glycine, α-glycine, glycine HCl and diglycine HCl (42); and laboratory XRD pattern of sodium glycinate are provided. The results are summarized in Table II.

Frozen solutions—10% w/v initial glycine concentration. In all frozen solutions the presence of crystalline hexagonal ice was evident from lines with d-spacings of 3.93, 3.65, 3.46 and 2.68 Å (Fig. 2). In the pH range 4.0–9.0, the β-glycine was observed in the frozen solutions (Fig. 2). Interestingly, at pH values of 4 and 5, diglycine HCl was also detected. Notably, γ-glycine was not detected in the frozen solutions in the pH range of 1.5 to 10. In glycine solutions under ambient conditions and during spray drying, γ-glycine crystallized from initial acidic (pH 3–4) as well as basic (pH 8–9) conditions (17,27). In our experiments using the laboratory XRD, the detection of low levels of γ-glycine would have been challenging in the presence of highly intense ice peaks (33). Notably, crystallization of glycine polymorph and salts can also be affected by the cooling rate, supersaturation levels, counter-ion concentration and the presence of ice (17,30). Therefore, it is possible that crystallization of diglycine HCl was favored kinetically during freezing. Moreover, it is known that crystallization of glycine at extreme pH conditions is slow and requires longer time to complete crystallization, as compared to neutral glycine solutions (17,27,30). Consequently, most of the glycine remained uncrystallized in the freeze-concentrate. If seeds or low levels of crystalline γ-glycine were present, but not detected, it should be evident upon crystallization during annealing or after drying. Naturally, our next step was to study the freeze-dried samples of 10% w/v glycine solutions.

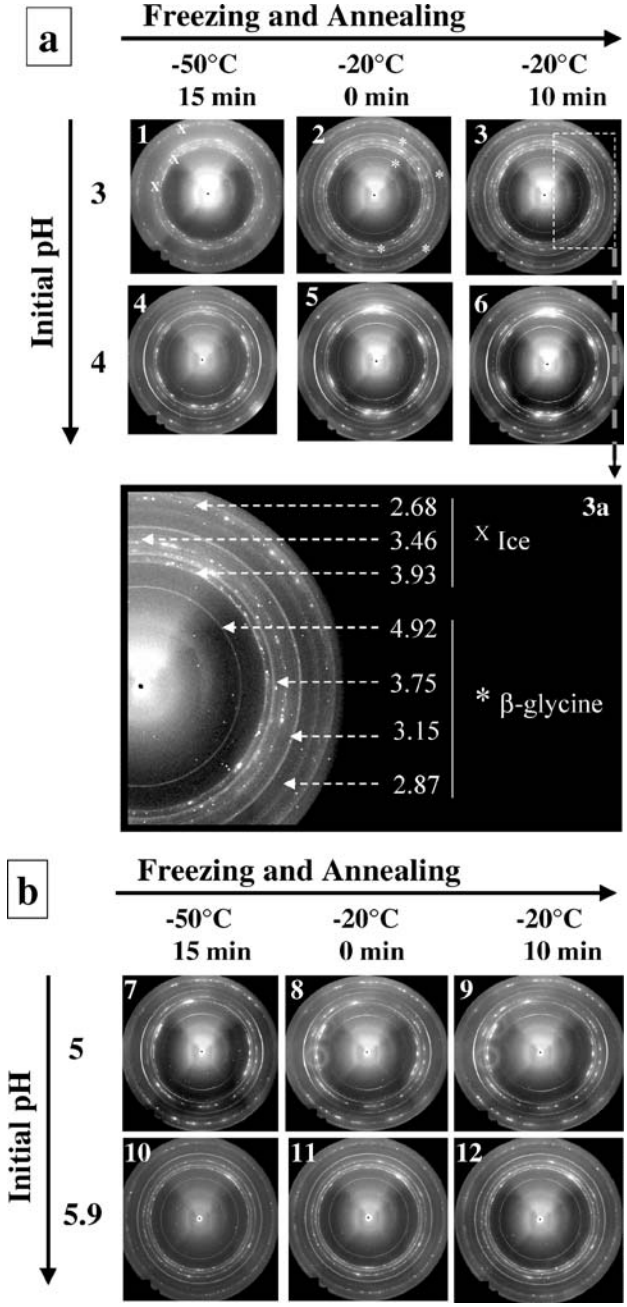

Fig. 6. 2D-SXRD patterns (Frame 1 to 12 in a and b) of *frozen solutions* of glycine at different stages of freezing and annealing. Glycine solutions (2% w/v) with initial solution pH in the range of 3 to 5.9 were cooled at 10°C/min from RT to −50°C, held for 15 min, then heated at 5°C/min to −20°C and annealed for 10 min. The characteristic lines for crystalline β-glycine are marked by *asterisk*, whereas the lines for crystalline ice are marked by ^{X}. For clarity, these lines are marked only in the frame 3a.

Lyophiles—10% w/v initial glycine concentration. When the solutions were freeze-dried using the bench-top lyophilizer, γ-glycine was detected when the initial solution pH was 3 and ≥8 (Fig. 3). The possible reasons for the crystallization of γ-glycine were discussed earlier. Additionally, the β→γ transition during freeze-drying cannot be ruled out (28–30). Pyne *et al.* observed this transition in the quench-cooled samples of neutral glycine solutions containing a mixture of β- and γ-glycine. Upon annealing at −10°C for ~4 h, the β→γ transition was complete (30). In our case, we could have obtained mixtures of β- and γ-glycine, not through quench cooling, but due to the initial solution pH. In glycine solutions, with initial pH values of 3, 8 or 9, while the pH may favor the formation of γ-glycine, the kinetic factors (e.g., ice crystallization) during freezing could produce β-glycine or diglycine HCl. Moreover, β→γ transition is possible during freeze-drying as the γ-polymorph (thermodynamically most stable) would be favored over the metastable β-polymorph. At high pH values of 9 and 10, sodium glycinate was detected in the lyophile. Again, the detection of this phase might have been a challenge in the frozen state when analyzed using a laboratory diffractometer.

Lyophiles—2 and 0.25% w/v initial glycine concentrations. Our next interest was to evaluate the effect of pH and low solute concentration upon the glycine phase crystallizing in the final lyophile. Therefore, maintaining a constant cooling rate (1°C/min), the effect of solution pH (range 1.5 to 10) and initial glycine concentration (2.0 and 0.25% w/v) were investigated (Figs. 4 and 5). We hypothesize that in the pH range of 3 to 8, during cooling, if the initial glycine concentration is decreased (lower supersaturation compared to 10% w/v solutions), the crystallization of β-glycine would be favored over γ-glycine. The rate of glycine crystallization during cooling, from solutions with initial pH values of 3 or 10, was slower than that from neutral solutions. The crystallization of γ-glycine occurred slowly whereas β-glycine crystallized rapidly in the presence of ice (17,27–29). Thus, a decrease in the crystallization rate of γ-glycine might allow the kinetically stable β-glycine to crystallize spontaneously. Moreover, there are no reports in the literature to suggest the inhibition of β-glycine

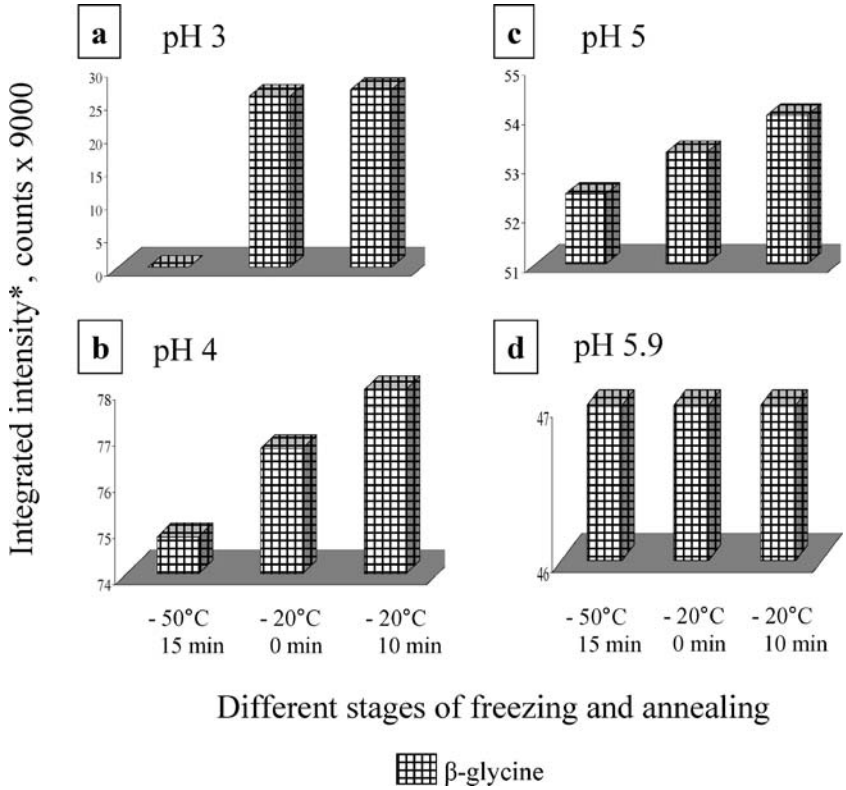

Fig. 7. Histograms displaying the intensities of peaks of β-glycine at different stages of freezing and annealing. The extent of crystallization of glycine is demonstrated as a function of initial solution pH: (a) 3, (b) 4, (c) 5 and (d) 5.9. In each case, glycine solutions (2% w/v) were cooled at 10°C/min from RT to −50°C, held for 15 min, then heated at 5°C/min to −20°C and annealed for 10 min. *Asterisk*: Sum of the integrated intensities of the characteristic peaks of β-glycine with d-spacing (Å): 3.15, 3.74, 4.92 (not included in (a)), 2.87(not included in c and d). Note the pronounced difference in the y-axis scale between panel (a) and panels (b–d).

(zwitterion) crystallization by charged glycine species ($^{+}H_3NCH_2COOH$ or $NH_2CH_2COO^{-}$) so as to favor γ-glycine formation. At ambient conditions, inhibition of α-glycine crystallization in solutions with initial pH values of 3 or 9 was explained to occur via 'self-poisoning' mechanism to produce γ-glycine (17). A crystal packing examination of α-glycine indicates that the hydrogen-bonded cyclic dimer (packed in two-dimensional array) is the building-block for the growth of α-glycine. The charged species of glycine inhibit the formation of the α-glycine dimers and consequently γ-glycine crystallizes in one-dimension polar chains (17,18). Interestingly, β-glycine exists as hydrogen-bonded monomers.

As expected, β-glycine was detected, along with γ-glycine, at pH 3. This is one of the few instances wherein a mixture of glycine polymorphs were obtained when a frozen solution, obtained by controlled cooling, was dried. Similarly at pH 8, when the glycine concentration was reduced from 2.0 to 0.25% w/v, β-glycine was detected.

Crystallization of glycine HCl and diglycine HCl in frozen solutions and lyophiles. At initial solution pH of 1.5 and 2, crystallization of diglycine HCl and/or glycine HCl was observed in the frozen solution as well as in the final lyophiles (Table II). In the pH range of 3 to 5, irrespective of the initial glycine concentration, diglycine HCl crystallized in the frozen solutions as well as in the lyophiles. A possible explanation is that after ice crystallization there was an increase in the chloride ion concentration in the freeze-concentrate, which facilitated the formation of diglycine HCl. Interestingly, Yu and Ng spray-dried the glycine solutions and demonstrated the formation of diglycine HCl as a minor component at pH 3 but not at pH 4 (27). The absence of diglycine HCl at pH 4 can be explained by the loss of HCl during the spray-drying process. In contrast, the freeze-drying process would retain most of the HCl, thereby favoring the formation of diglycine HCl. In contrast to our use of SXRD, previous studies had utilized a laboratory XRD wherein the diglycine HCl may not have been detected. In this context, SXRD is an excellent technique for unambiguous identification and quantification of multiple phases.

Extent of Glycine Crystallization in Frozen Solutions—pH and Annealing Effects

Our interest was to focus in the pH range 3 to 5.9, where multiple crystalline glycine phases were predominantly detected. We anticipated that the high sensitivity of SXRD would permit quantification of glycine phases even at a low initial solute concentration of 2% (266 mM). Since we also intended to investigate the effect of annealing, a high cooling

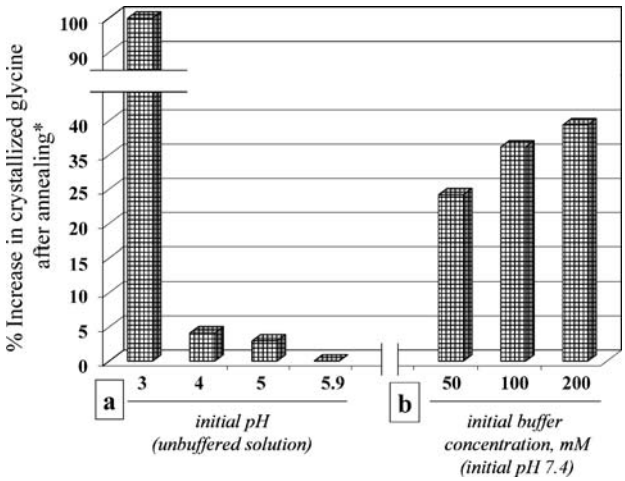

Fig. 8. Extent of glycine crystallization upon annealing; (a) over the initial solution pH range of 3.0 to 5.9; (b) at buffer concentrations of 50, 100 and 200 mM in glycine–phosphate buffer solutions (initial pH of 7.4). *Asterisk*:Assuming that annealing for 10 min at −20°C caused complete solute crystallization (i.e., 100% crystalline glycine).

rate of 10°C/min was chosen. A high cooling rate would favor retention of glycine in the amorphous state, which would then crystallize upon annealing. At a fixed cooling rate, the physical form of glycine in the freeze-concentrate will be dictated by the initial solution pH (17,27–29). Hence, we were able to determine the effect of initial pH on the glycine phase crystallizing from solution and then determine the effect of annealing on the extent of solute crystallization.

In all cases, in addition to hexagonal ice, β-glycine was detected (Fig. 6). The effect of initial solution pH on the extent of glycine crystallization is readily evident by comparing the 2D-SXRD patterns obtained at −50°C (Frame 1, 4, 7 and 10 in Fig. 6). In Fig. 7, the first bar in each panel displays the corresponding integrated intensities of β-glycine peaks. The absolute intensities of the peaks of hexagonal ice (major phase, not shown in Fig. 7) varied from sample to sample. Therefore, in the absence of an internal standard, it is inappropriate to compare the *integrated intensities* across samples of different initial pH values. Only the relative intensities (not shown in Fig. 7) could be compared.

The effect of annealing is most pronounced when the initial solution pH was 3. This effect can be discerned by comparing the 2D-SXRD patterns in frames 1 to 3 in Fig. 6. There was substantial glycine crystallization when the frozen solution was heated from −50 to −20°C. However, holding at the annealing temperature caused a small increase in crystalline glycine content (Fig. 7a). In contrast, when solutions of pH 4 and 5 were cooled to −50°C, glycine crystallization was readily evident. Annealing at −20°C caused a modest increase in crystalline glycine content. Starting with initial solution pH of 5.9, there was substantial glycine crystallization at −50°C, and heating to −20°C and annealing caused no change in the peak intensities of glycine.

In all cases, there was no change in the integrated intensities of peaks of crystalline glycine after annealing for 10 or 20 min. For the sake of clarity, the 2D-SXRD patterns obtained after annealing for 20 min are not shown in Figs. 7, 8, 9 and 10. At all pH values, assuming that annealing causes complete crystallization of glycine, it is possible to calculate the percent increase in crystalline glycine due to annealing (Fig. 8a). Annealing solutions of pH values 5.9, 5.0 and 4.0 resulted in an increase in crystalline glycine content by 0, 3.0 and 4.1%, respectively. For glycine solution with initial pH of 3, *all* of the crystallization could be attributed to annealing.

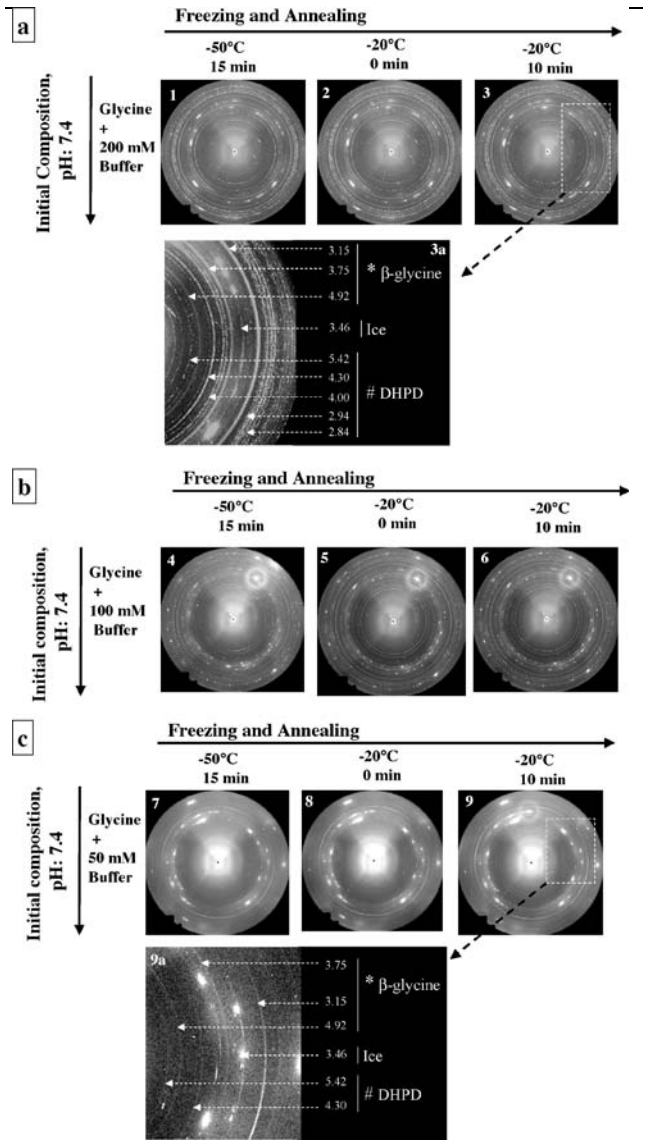

Fig. 9. 2D-SXRD patterns (Frame 1 to 9 in a, b, c) of *frozen solutions* of glycine and sodium phosphate buffer (initial solution pH 7.4) at different stages of freezing and annealing. In each case, the initial glycine concentration was 266 mM. The buffered glycine solutions were cooled at 2°C/ min from RT to −50°C, held for 15 min, then heated at 5°C/min to −20°C and annealed for 10 min. Selected characteristic lines of β-glycine are marked by (*asterisk*), whereas the lines of DHPD are marked by (#). For clarity, these lines are shown only in the frame 3a and 9a.

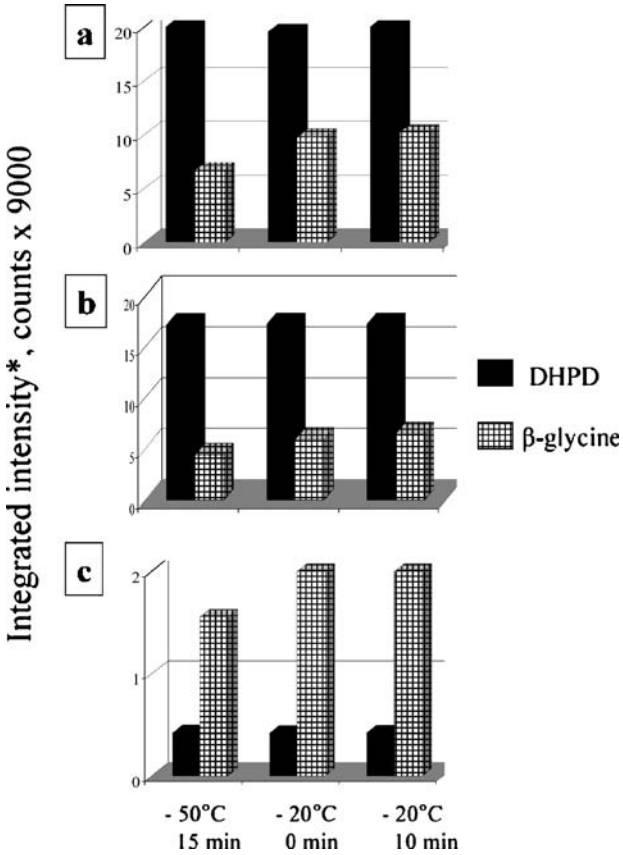

Fig. 10. Histograms displaying the intensities of peaks of β-glycine and DHPD at different stages of freezing and annealing. The extent of crystallization of glycine and buffer salt is shown as a function of initial solution composition. In the solution the glycine concentration was 266 mM and the buffer concentration was (a) 200 mM, (b) 100 mM and (c) 50 mM. All the solutions with initial pH of 7.4 were cooled at 2°C/min from RT to −50°C, held for 15 min, then heated at 5°C/min to −20°C and annealed for 10 min. *Asterisk*: Sum of the integrated intensities of the characteristic peaks with d-spacing (Å): 4.92 for β-glycine and 5.42 for DHPD (41,42).

Extent of Crystallization of Glycine—Effect of Buffer Concentration

Our next interest was to investigate whether changes in the pH caused by the crystallization of buffer salt could also affect the extent or polymorphic outcome of crystalline glycine. We hypothesize that such effects would be evident at phosphate buffer concentrations ≥50 mM where maximum crystallization of DHPD or highest pH shifts have been observed (29,30). In the current study, the effect of annealing on the extent of glycine crystallization was monitored at phosphate buffer concentrations of 50, 100 and 200 mM. In a subsequent investigation (the subject of a future manuscript), we have evaluated multi-component systems at buffer concentrations in the range of 1 to 50 mM.

SXRD permitted simultaneous identification of multiple crystalline phases. It was also possible to quantify the effect of annealing on the solute crystallization in the frozen solutions (Figs. 8, 9 and 10). In all frozen solutions, besides hexagonal ice, crystallization of disodium hydrogen phosphate dodecahydrate (DHPD) and β-glycine was evident (Fig. 9). As expected, with a decrease in the initial buffer concentration, there was a decrease in crystalline DHPD content. This is evident by comparing the 2D-SXRD patterns in frames 1, 4 and 7 obtained at −50°C (Fig. 9).

The intensities of the 4.92 Å line of β-glycine and 5.42 Å line of DHPD formed the basis of their quantification (Fig. 10). DHPD crystallization was complete at −50°C. The crystallization of glycine was inhibited by the phosphate buffer. This was evident from the increase in crystalline glycine peak intensity when the temperature was raised from −50°C to the annealing temperature of −20°C. Interestingly, holding at −20°C for 10 min did not cause any further increase in the peak intensities. Phosphate buffer exhibited a concentration dependent inhibition of glycine crystallization (Fig. 8b). At buffer concentrations of 200, 100 and 50 mM, the increase in the crystalline glycine content following annealing were 34, 31 and 24%, respectively.

Pikal-Cleland *et al.* had evaluated in detail the effect of glycine on the pH shift of phosphate buffer during freezing. At glycine concentrations <50 mM, the pH shift of phosphate buffer was suppressed, while at glycine concentrations >100 mM, there was more complete crystallization of DHPD. Moreover, at glycine concentrations ≤100 mM and at 100 mM buffer concentration, glycine crystallization was not observed. This conclusion was based on DSC studies wherein the solutions were cooled to −30°C at 20°C/min. This was attributed to the possible formation of sodium glycinate though they were unable to detect it by DSC (14).

In our systems, while maintaining a constant glycine concentration (266 mM), we have determined the effect of phosphate buffer concentration, over the range of 50 to 200 mM, on the crystallization of both glycine and DHPD. Our cooling rate was 2°C/min, and we cooled the solutions down to −50°C. In order to facilitate solute crystallization, our systems were also annealed at −20°C for 10 min. The glycine concentrations in our studies were much higher, and SXRD enabled direct identification of the phases crystallizing from solution. As the buffer concentration increased, the extent of glycine crystallization in the frozen solution decreased. This was evident from the pronounced increased in the crystalline glycine content upon annealing (Fig. 10). However, in all cases, only β-glycine was observed and there was no evidence of sodium glycinate formation. This is not surprising, considering the fact that sodium glycinate was observed only from solutions of pH ≥ 8 (Table II). The solution phase equilibria of the different forms of glycine have been elaborated by Towler *et al.* (17). Between the pH values of 2.39 and 9.78, glycine exists in the zwitterionic form. Thus, sodium glycinate formation is not favored at pH < 7.4. Moreover, with buffer salt crystallization, the actual pH in the freeze-concentrated solution is expected to be substantially lower.

SIGNIFICANCE

The effect of initial solution pH, over the range of 1.5 to 10, on the salt and polymorphic forms of glycine crystallizing in frozen solutions, and upon lyophilization of these solutions, has been systematically demonstrated. In the lyophiles, in addition to two polymorphic forms of glycine, β- and γ-

glycine, three salts, glycine HCl, diglycine HCl, and sodium glycinate were identified. Importantly, in the pH range of 3–5, binary mixtures of glycine polymorphs, glycine—diglycine HCl and ternary mixture of glycine polymorphs and diglycine HCl were obtained. The use of synchrotron radiation allowed the unambiguous identification of the multiple crystalline phases.

As the initial solution pH (unbuffered systems) decreased from 5.9 to 3, there was a dramatic decrease in glycine crystallization in the frozen system. The crystallization of glycine on annealing was monitored *in situ*, in the synchrotron beamline. In phosphate buffered solutions, our results provided an indirect measure of the pH shift in the freeze concentrate when it was cooled to −50°C. The selective crystallization of DHPD is reported to shift the pH towards the acidic side, by 2–3 units, from the initial pH of 7.4. As the buffer concentration is increased, the shift is more pronounced (4,24,25). Taking the 50 mM phosphate buffered system as an example (Figs. 8b and 10), the glycine crystallization was incomplete when the solutions were cooled to −50°C. There was a pronounced increase in the crystalline glycine content when the system was heated to the annealing temperature. The pH shift in the freeze-concentrate could explain this incomplete glycine crystallization. The pH shift is also supported by the crystallization of DHPD (Fig. 10). As the buffer concentration was increased, first to 100 and then to 200 mM, the more pronounced pH shift is expected to result in more incomplete glycine crystallization. This was manifested by the increase in crystalline glycine content following annealing (Figs. 8b and 10).

While the glycine-phosphate buffer was used as a model system, SXRD can be utilized to detect solute crystallization and to evaluate extent of crystallization of other bulking agents and buffer salts of pharmaceutical interest. Although no API was utilized in our study, the presence of crystalline or amorphous API (e.g., protein) can influence the form and extent of crystallization of glycine and/or buffer salts during freeze-drying cycle. SXRD is particularly useful for the characterization of multi-component systems with several crystalline phases. Moreover, the entire freeze-drying cycle can be carried out in the sample chamber and phase transitions *during* each stage of the process can be monitored. Therefore, high sensitivity of SXRD, coupled with the *in situ* freeze-drying technique, can enable the development of robust freeze-dried formulations. We are currently investigating the utility of SXRD to study such systems, and specifically protein formulations.

CONCLUSIONS

The pH and solute concentration of the solutions prior to lyophilization affected the salt and polymorphic forms of glycine crystallizing in frozen solutions and in lyophiles. The extent of glycine crystallization in frozen solutions was influenced by the pH and phosphate buffer concentration. Synchrotron XRD is a useful tool for simultaneous detection and quantification of multiple crystalline phases.

ACKNOWLEDGMENTS

The authors thank Dr. Douglas Robinson of Midwestern Collaborative Access Team for the beam-line management and valuable support during the experiments. This work was supported, in part, by a Research Challenge award from the Ohio Board of Regents and from the National Science Foundation grant DMR-0312792. Use of the Advanced Photon Source (APS) was supported by the US Department of Energy, Basic Energy Sciences, Office of Science, under contract no. W-31-109-Eng- 38. The Midwest Universities Collaborative Access Team (MUCAT) sector at the APS is supported by the US Department of Energy, Basic Energy Sciences, Office of Science, through the Ames Laboratory under contract no. W-7405-Eng-82. We thank Linda Sauer for her assistance in setting up the instrumentation. Any opinions, findings, and conclusions or recommendations expressed in this publication are those of the author(s) and do not necessarily reflect the views of the National Science Foundation.

REFERENCES

1. M. J. Pikal. Freeze Drying. In J. Swarbrick and J. C. Boylan (eds.), *Encyclopedia of Pharmaceutical Technology*, Marcel Dekker, New York, 2002, pp. 1299–1326.
2. L. A. Trissel. *Handbook of Injectable Drugs*, ASHP, Bethesda, MD, 1994.
3. X. Tang and M. J. Pikal. Design of freeze-drying processes for pharmaceuticals: practical advice. *Pharm. Res.* **21**:191–200 (2004).
4. J. F. Carpenter, B. S. Chang, W. Garzon-Rodriguez, and T. W. Randolph. Rational design of stable lyophilized protein formulations: theory and practice. In J. F. Carpenter and M. C. Manning (eds.), *Rational design of stable lyophilized protein formulations*: *theory and practice*, Plenum, New York, 2002, pp. 109–133.
5. T. W. Randolph. Phase separation of excipients during lyophilization: effects on protein stability. *J. Pharm. Sci.* **86**:1198–1202 (1997).
6. E. Y. Shalaev, F. Franks, and P. Echlin. Crystalline and amorphous phases in the ternary system water–sucrose–sodium chloride. *J. Phys. Chem.* **100**:1144–1152 (1996).
7. E. Y. Shalaev. The impact of buffer on processing, and stability of freeze-dried dosage forms, part 1: solution freezing behavior. *Amer. Pharm. Rev.* **8**:80–87 (2005).
8. J. F. Carpenter, M. J. Pikal, B. S. Chang, and T. W. Randolph. Rational design of stable lyophilized protein formulations: some practical advice. *Pharm. Res.* **14**:969–975 (1997).
9. X. Li and S. L. Nail. Kinetics of glycine crystallization during freezing of sucrose/glycine excipient systems. *J. Pharm. Sci.* **94**:625–631 (2005).
10. K. Chatterjee, E. Y. Shalaev, and R. Suryanarayanan. Partially crystalline systems in lyophilization: I. Use of ternary state diagram to determine extent of crystallization of bulking agent. *J. Pharm. Sci.* **94**:798–808 (2005).
11. E. Y. Shalaev, D. V. Malakhov, A. N. Kanev, V. I. Kosyakov, F. V. Tuzikov, N. A. Varaksin, and V. J. Vavillin. Study of the phase diagram water fraction of the system water—glycine—sucrose by DTA and X-ray methods. *Thermochim. Acta* **196**:210–220 (1992).
12. A. Pyne, K. Chatterjee, and R. Suryanarayanan. Solute crystallization in mannitol–glycine systems—implications on protein stabilization in freeze-dried formulations. *J. Pharm. Sci.* **92**: 2272–2283 (2003).
13. J. S. Searles, J. F. Carpenter, and T. W. Randolph. Annealing to optimize the primary drying rate, reduces freezing–induces drying rate heterogeneity, and determine Tg' in pharmaceutical lyophilization. *J. Pharm. Sci.* **90**:872–887 (2001).
14. K. A. Pikal-Cleland, J. L. Cleland, T. J. Anchordoquy, and J. F. Carpenter. Effect of glycine on pH changes and protein stability during freezing–thawing in phosphate buffer systems. *J. Pharm. Sci.* **91**:1969–1979 (2002).
15. L. van den Berg. pH changes in buffers and foods during freezing and subsequent storage. *Cryobiology* **3**:236–242 (1966).

16. L. van den Berg and D. Rose. Effect of freezing on the pH and composition of sodium and potassium phosphate solutions: The reciprocal system: KH_2PO_4–Na_2HPO_4–H_2O. *Arch. Biochem. Biophys.* **81**:319–329 (1959).
17. C. S. Towler, R. J. Davey, R. W. Lancaster, and C. J. Price. Impact of speciation on crystal nucleation in polymorphic systems: the conundrum of γ glycine and molecular 'self poisoning'. *J. Am. Chem. Soc.* **126**:13347–13353 (2004).
18. I. Weissbuch, V. Y. Torbeev, L. Leiserwitz, and M. Lahav. Solvent effects on crystal polymorphism: why addition of methanol or ethanol to aqueous solutions induces the precipitation of the least stable β form of glycine. *Angew. Chem., Int. Ed.* **44**:3226–3229 (2005).
19. E. S. Ferrari, R. J. Davey, W. I. Cross, A. L. Gillon, and C. S. Towler. Crystallization in polymorphic systems: the solution-mediated transformation of β to α glycine. *Cryst. Growth Des.* **3**:53–60 (2003).
20. E. V. Boldyreva, V. A. Drebushchak, T. N. Drebushchak, I. E. Paukov, Y. A. Kovalevskaya, and E. S. Shutova. Polymorphism in glycine. Thermodynamic aspects. Part I. Relative stability of the polymorphs. *J. Therm. Anal. Calorim.* **73**:409–418 (2003).
21. H. Sakai, H. Hosogai, and T. Kawakita. Transformation of α-glycine to γ-glycine. *J. Cryst. Growth* **116**:421–426 (1992).
22. B. A. Garetz, J. Matic, and A. S. Myerson. Polarization switching of crystal structure in the nonphotochemical light-induced nucleation of supersaturated aqueous glycine solutions. *Phys. Rev. Lett.* **89**:1755501-1-4, 2002 (2002).
23. A. Ito, M. Yamanobe-Hada, and H. Shindo. *In situ* AFM observation of polymorphic transformation at crystal surface of glycine. *J. Cryst. Growth* **275**:e1691–e1995 (2005).
24. G. L. Perlovich, L. K. Hansen, and A. Bauer-Brand. The polymorphism of glycine. Thermochemical and structural aspects. *J. Therm. Anal. Calorim.* **66**:699–715 (2001).
25. E. S. Ferrari, R. J. Davey, W. I. Cross, A. I. Gillon, and C. S. Towler. Crystallization in polymorphic systems: the solution-mediated transformation of β to α glycine. *Cryst. Growth. Des.* **3**:53–60 (2003).
26. T. D. Davis, G. E. Peck, J. G. Stowel, K. R. Morris, and S. R. Byrn. Modeling and monitoring of polymorphic transformations during the drying phase of wet granulation. *Pharm. Res.* **21**:860–866 (2004).
27. L. Yu and K. Ng. Glycine crystallization during spray drying: the pH effect on salt and polymorphic forms. *J. Pharm. Sci.* **91**:2367–2375 (2002).
28. M. J. Akers, N. Milton, S. R. Byrn, and S. L. Nail. Glycine crystallization during freezing: the effects of salt form, pH, and ionic strength. *Pharm. Res.* **12**:1457–1461 (1995).
29. S. Chongprasert, S. A. Knopp, and S. L. Nail. Characterization of frozen solutions of glycine. *J. Pharm. Sci.* **90**:1720–1728 (2001).
30. A. Pyne and R. Suryanarayanan. Phase transitions of glycine in frozen aqueous solutions and during freeze-drying. *Pharm. Res.* **18**:1448–1454 (2001).
31. G. Gomez, M. J. Pikal, and N. Rodriguez-Hornedo. Effect of initial buffer composition on pH changes during far-from equilibrium freezing of sodium phosphate buffer solutions. *Pharm. Res.* **18**:90–97 (2001).
32. G. Gomez. *Crystallization-related pH changes during freezing of sodium phosphate buffer solutions*, Ph.D. Dissertation, University of Michigan, Ann Arbor, Michigan, 1995.
33. D. B. Varshney, S. Kumar, E. Y. Shalaev, S. W. Kang, L. A. Gatlin, and R. Suryanarayanan. Solute crystallization in frozen systems—use of synchrotron radiation to improve sensitivity.- *Pharm Res.* **46**:41–47 (2006).
34. R. Govindarajan, K. Chatterjee, L. Gatlin, R. Suryanarayanan, and E. Y. Shalaev. Impact of freeze-drying on ionization of sulfonephthalein probe molecules in trehalose–citrate systems. *J. Pharm. Sci.* **95**:1498–1510 (2006).
35. N. Blagden, R. Davey, M. Song, M. Quayle, S. Clark, D. Taylor, and A. Nield. A novel batch cooling crystallization for *in situ* monitoring of solution crystallization using energy dispersive X-ray diffraction. *Cryst. Growth Des* **3**:197–201 (2003).
36. C. Nunes. *Use of High-Intensity X-Radiation in Solid-State Characterization of Pharmaceuticals*, Ph.D. Dissertation, Department of Pharmaceutics, University of Minnesota, 2005.
37. C. Nunes, A. Mahendrasingam, and R. Suryanarayanan. Quantification of crystallinity in substantially amorphous materials by synchrotron X-ray powder diffractometry. *Pharm. Res.* **22**:1942–1953 (2005).
38. A. P. Hammersley. *ESRF internal report*, ESRF97HA02T, "Fit2D: an introduction and overview", (1997).
39. A. P. Hammersley, S. O. Svensson, M. Hanfland, A. N. Fitch, and D. Häusermann. Two-dimensional detector software: from real detector to idealized image or two-theta scan. *High Press. Res.* **14**:235–248 (1996).
40. Powder Diffraction File. (hexagonal ice, PDF-2, Card #00-042-1142), International Centre for Diffraction Data, Newtown Square, PA, 1996.
41. Powder Diffraction File. (disodium hydrogen phosphate dodecahydrate, PDF-2, Card #00-011-0657), International Centre for Diffraction Data, Newtown Square, PA, 1996.
42. Powder Diffraction File. (glycine polymorphs and salts, α-glycine ($^+H_3NCH_2CO_2^-$), PDF-2, Card #00-32-1702; β-glycine ($^+H_3NCH_2CO_2^-$), PDF-2, Card #00-002-0171; γ-glycine ($^+H_3NCH_2CO_2^-$) PDF-2, Card #00-006-0230; glycine hydrochloride ($^+H_3NCH_2CO_2H{\cdot}Cl^-$), PDF-2, Card #00-022-1744; diglycine hydrochloride ($^+H_3NCH_2CO_2^-{\cdot}{}^+H_3NCH_2CO_2H{\cdot}Cl^-$), PDF-2, Card #00-032-1649), International Centre for Diffraction Data, Newtown Square, PA, 1996.